RSC
Applied Interfaces

rsc.li/RSCApplInter

ROYAL SOCIETY
OF CHEMISTRY

PAPER
Hiroshi Yabu *et al.*
Rare-metal-free high-performance water-activated
paper battery: a disposable energy source for wearable
sensing devices

PAPER

Check for updates

Rare-metal-free high-performance water-activated paper battery: a disposable energy source for wearable sensing devices†

Kosuke Ishibashi, [iD] [a] Shimpei Ono, [iD] [b] Jun Kamei, [c] Koju Ito [d] and Hiroshi Yabu [iD] *[ad]

Lightweight, thin paper-based devices are attracting attention due to their portability, lower metal and plastic use, and smaller environmental impact when discarded. For example, paper-based thin diagnostic devices can be mass-produced and their environmental impact after disposal is low, making them promising rapid diagnostic devices for diseases and infectious diseases, especially in developing countries. This report describes a high-performance paper battery activated by water composed of a Mg–air battery with a neutral electrolyte and a safe, high-performance pigment-based electrocatalyst. The paper battery was fabricated by bonding Mg foil to paper and forming a cathode catalyst and gas diffusion layer (GDL) directly on the opposite surface. The fabricated paper battery achieved an OCV of 1.8 V, a 1.0 V current density of 100 mA cm^{-2}, and a maximum output of 103 mW cm^{-2}. The safety of materials used in the paper battery was also examined. Furthermore, applications of the battery in wearable sensing devices, such as a pulse oximeter (SpO$_2$ sensor) and a GPS logger, were also demonstrated.
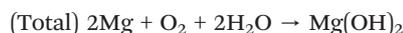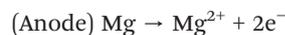
Introduction

In recent years, energy devices have to meet more than just high-performance standards like power and capacity; they also need to be environmentally friendly.[1,2] Among natural processes, the pinnacle of energy conversion efficiency is exemplified by the photosynthetic mechanism inherent in plants. During the daytime, plants utilize solar energy to synthesize sugars from water drawn from the ground and carbon dioxide from the air, fix this energy, and maintain life by extracting energy from the stored sugars through respiration. Applying this relationship to artificial energy devices, photosynthesis and respiration can be seen as analogous to the charging and discharging processes in batteries.

The respiratory system in plants, facilitated by transpiration, gas exchange in leaves, and the associated capillary forces in the xylem, is highly sophisticated and

serves as a valuable model for devices that obtain energy with low environmental impact. Efforts have been made to mimic photosynthesis through technologies like photovoltaic solar cells or artificial photosynthesis, which directly convert sunlight into electricity. In contrast, respiration, which is essential for sustaining plant life and involves the synthesis of the energy currency ATP from substrates like sugars, is analogous to the discharge process in batteries but has received less attention. If an energy device inspired by the respiration process in plants could be realized, it might offer the potential to extract significant energy with low environmental impact.

This leads us to focus on metal–air batteries, particularly magnesium–air batteries, which generate power using the same oxygen and water by using magnesium as a substrate. A magnesium–air battery is composed of the following reactions:

$$\text{(Anode) } Mg \rightarrow Mg^{2+} + 2e^-$$

$$\text{(Cathode) } O_2 + 2H_2O + 4e^- \rightarrow 4OH^-$$

$$\text{(Total) } 2Mg + O_2 + 2H_2O \rightarrow Mg(OH)_2$$

Except for the use of sugars as a substrate and the resulting energy being ATP, the utilization of oxygen and water is similar to respiration in plants. However, magnesium–air

[a] *Advanced Institute for Materials Research (WPI-AIMR), Tohoku University, 2-1-1, Katahira, Aoba-Ku, Sendai 980-8577, Japan. E-mail: hiroshi.yabu.d5@tohoku.ac.jp*

[b] *Central Research Institute of Electric Power Industry (CRIEPI), 2-6-1 Nagasaka, Yokosuka-shi, Kanagawa 240-0196, Japan*

[c] *AMPHIBIO, Ltd., Makerversity, West Goods Entrance, Somerset House, Victoria Embankment, London, WC2R 1LA, UK*

[d] *AZUL Energy, Inc., 1-9-1, Ichibancho, Aoba-Ku, Sendai 980-0811, Japan*

† Electronic supplementary information (ESI) available: Catalyst performances, design of devices, EIS data, and other paper battery cells' performances. See DOI: https://doi.org/10.1039/d4lf00039k

batteries face challenges as they use heavy metals like manganese oxide as oxygen reduction catalysts and because magnesium is highly soluble in water, making it difficult to construct battery cells. Therefore, in order to make the magnesium–air battery a device that can be used practically, it is necessary to construct a system that supplies electrolytes and uses an oxygen reduction catalyst with low environmental impact.

In general, for conventional metal–air batteries, the anode material should remain in a stable solid state in an electrolyte during storage and should dissolve in the electrolyte with starting discharge. For example, in Zn–air batteries, Zn does not dissolve immediately when placed in alkaline aqueous electrolytes. It remains stable in the electrolyte until the circuit is connected to the battery, and it dissolves during discharge. On the other hand, it is well known that Mg dissolves in a neutral aqueous electrolyte at room temperature. Therefore, the Mg anode cannot be stored in the cell state with the neutral electrolyte.

Lightweight, thin paper-based devices are attracting attention due to their portability, lower metal and plastic use, and smaller environmental impact when discarded. In particular, batteries that use aqueous electrolytes are useful as power generation devices triggered by water due to the capillary property of paper,[3,4] and paper-based fuel cells using hydrogen peroxide and formic acid[3] and biofuel cells[5–7] have been proposed. Furthermore, metal–air batteries for emergency power sources and water leakage sensors using paper as the water suction layer have been commercialized. Paper-based Al–air and Zn–air batteries that use strong alkaline aqueous electrolytes have been reported with power densities of up to 100 mW cm^{-1}.[4,8–10] We thought that if a system in which paper absorbs electrolyte by capillary force, like plants suck up water from the ground, could be applied to magnesium–air batteries, the problem of magnesium dissolving in the electrolyte and self-discharging would be solved.

Furthermore, in metal–air batteries, the efficiency of the oxygen reduction reaction (ORR) at the cathode is the main factor determining the power generation efficiency. Neutral electrolytes are best, particularly for minimizing environmental impact and improving safety after disposal. However, because the ORR does not proceed easily under neutral conditions, an electrocatalyst that promotes the ORR efficiently in neutral electrolytes is required. Generally, Pt/C, in which Pt nanoparticles are supported on carbon, and inexpensive MnO_2 are used as electrocatalysts, but both contain heavy metals, and Pt nanoparticles are expensive and can ignite under dry conditions, making them unsuitable for paper-based devices. In particular, manganese compounds such as manganese dioxide are well-known heavy metals with reproductive toxicity (category 2), specific target organ toxicity (category 1), and aquatic environmental hazards (category 4) according to the GHS classification. Consequently, manganese batteries commonly available in Japan cannot be simply disposed of and are mandated to be collected for recycling and not to be exposed to the outer environment. Of course, even if a material has high performance, Pt, which poses environmental hazards and fire risks, cannot be used in paper batteries. Therefore, it is necessary to develop an electrocatalyst that is inexpensive, safe, and sustainable, and has high ORR activity as a cathode in neutral electrolytes.

Carbon alloy catalysts containing various heteroatoms, such as N and FeN_4 structures, as catalytically active sites in the carbon network have been reported,[11–15] some of which exhibit high activity close to that of Pt/C.[16] However, the introduction of heteroatoms is difficult to control, and the process cost is high because of the use of high-temperature carbonization reactions of organic materials. In addition, few catalysts that exhibit sufficient performance in the neutral region have been reported. A Zn–air paper battery comprising zinc foil and carbon electrodes printed with commercial pigments on the surface of paper has been reported, and this battery generated electricity when it was activated by absorbing water.[17] However, the open circuit voltage (OCV) of the battery was less than 1.2 V, the output current was less than 1 mA cm^{-2}, and its power output was only about 150 μW cm^{-2}, and these values were not sufficient compared with a conventional Zn–air battery. The pigment iron phthalocyanine (FePc) has also been investigated as an electrocatalyst that has an FeN_4 structure, which is the catalytically active centre for the ORR,[18] but this type of electrocatalyst has generally shown insufficient ORR activity due to high aggregation. Catalysts with high ORR activity have been obtained by immobilizing FePc on highly conductive nanocarbons, such as CNTs, at the molecular level.[19] However, FePc is insoluble in solvents and aggregates easily, requiring high-temperature processes and modifications on the carbon side.

We have reported that AZUL catalysts with iron azaphthalocyanine (FeAzPc) molecularly adsorbed on carbon exhibit high ORR activity in alkaline and HCl acidic aqueous electrolytes.[20] It has been theoretically predicted that FeAzPc will exhibit higher ORR activity than FePc. Furthermore, FeAzPc showed high activity even when supported on commercially available Ketjen black (KB) and other carbon materials, and nanocarbons, such as CNTs, were not necessary.[21] The molar weight activity of FeAzPc as a cathode catalyst for metal–air batteries was also high.[22]

This paper reports the realization of a bio-inspired water-activated magnesium–air paper battery by using only low environmental impact materials and without use of heavy metals, by mimicking the energy generation system in plant respiration. The paper battery was fabricated by bonding Mg foil to paper and forming a cathode catalyst and gas diffusion layer (GDL) directly on the opposite surface. The fabricated paper battery achieved an OCV of 1.8 V, a 1 V current density of 100 mA cm^{-2}, and a maximum output of 103 mW cm^{-2}, values at least 700 times higher than those of previously reported paper batteries.[16] Additionally, under the optimal conditions, the maximum output power density reached 120 mW cm^{-2}. The safety of materials used in the paper battery

was also examined. Furthermore, applications of the battery in wearable sensing devices, such as a pulse oximeter (SpO₂ sensor) and a GPS logger, were also demonstrated.

Results and discussion

Fig. 1(a) shows the structure of the paper battery, which is a simple structure and consists of a cathode-current collector composite sandwiched between the water-absorbing paper and the anode. In this study, a Mg–air battery using Mg foil as the anode was fabricated because Mg is an abundant element in nature and easily dissolves in saltwater electrolytes, making it an ideal anode material for a saltwater-activated battery with low environmental impact. Catalyst ink (2.5 wt% catalyst) was prepared by mixing an AZUL electrocatalyst, 20% Nafion® dispersion in IPA, and deionized water in a planetary ball mill using zirconia balls and pots. It is noteworthy that the AZUL catalyst shows much higher ORR activities under neutral pH conditions than the MnO_2 catalyst, which is normally used as an electrocatalyst for metal–air batteries, and almost the same performance as Pt/C, which is normally used as a high-performance electrocatalyst for fuel cells and metal–air batteries (see the ESI,† S1). Mg foil was fixed onto the paper sheet, and then the back of the paper was coated with the catalyst ink by spray coating (Fig. 1(b)). Finally, the paper battery cell was fabricated by using a Cu mesh as a current collector as shown in Fig. 1(c).

The battery performance depends on the water absorbent paper. Three types of absorbent paper sheets, with densities of 0.56 (1), 0.46 (2), and 0.31 g cm⁻³ (3), were used (ESI,† S2). A current collector, cathode, and water absorbent paper sheet composite were prepared by applying an ink mixture consisting of the catalyst, carbon nanofibers (CNFs), and a binder to the paper sheet, placing a current collector mesh onto the sheet, and drying. The catalytic electrode area was 10 × 10 mm.

The white area in the photograph (Fig. 1(c)) was the uncoated paper and this area was exposed to the electrolyte solution to suck up the electrolyte solution into the active area of the battery. When this section was dipped into the electrolyte, the electrolyte was loaded by capillary force, initiating power generation.

Evaluating the effect of the current collector material (Ni or Cu) on the battery performance showed that a Cu mesh achieved a better performance (see the ESI,† S3). Because Cu has lower resistivity than Ni, the current was transferred more efficiently *via* the Cu mesh current collector.

Fig. 2(a) and (b) show the I–V and I–P polarization curves of the paper batteries measured in 4 M NaCl solution, respectively. Table 1 shows the density of the absorbent paper used, the battery properties (OCV, maximum power output (P_{max}), maximum current density (I_{max}), and capacity density), and the time taken for the batteries to start generating electricity. The OCVs of cells 1 and 2 were similar, but that of cell 3 was lower than that of cell 1. Cell 3 had the highest P_{max} and I_{max} values, achieving a maximum output of 103 mW cm⁻², which was approximately twice the output of a previously reported paper battery based on the Mg–air battery.[9] This result was attributed to the higher water retention property of the paper towel compared with other paper materials in previous paper batteries. Although the paper was thicker in the present work, it had a higher porosity, which facilitated the formation of the interface between the electrolyte and electrode and promoted efficient exchange of ions. Electrochemical impedance spectroscopy (EIS) showed that cell 1 had high electrolyte and cell resistance compared with cells 2 and cell 3, which indicated that higher resistivity was induced with the denser fiber network of the paper even though the capillary force was higher (ESI,† S6).
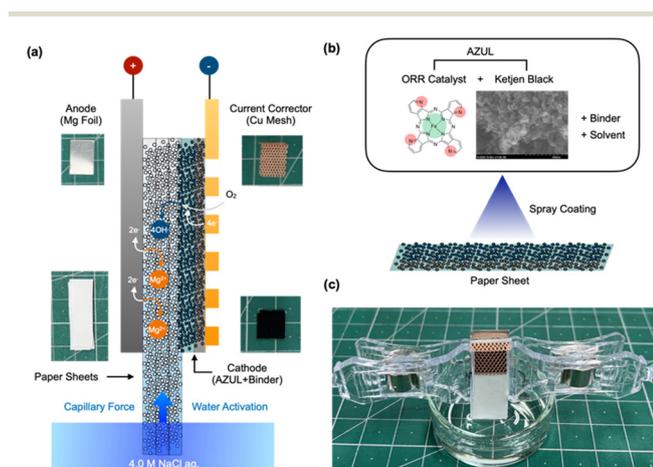

Fig. 1 Schematics of the water-activated paper-based battery cell (a) and cathode fabrication (b), and photograph of the water activation setup for battery performance evaluation (c), respectively.
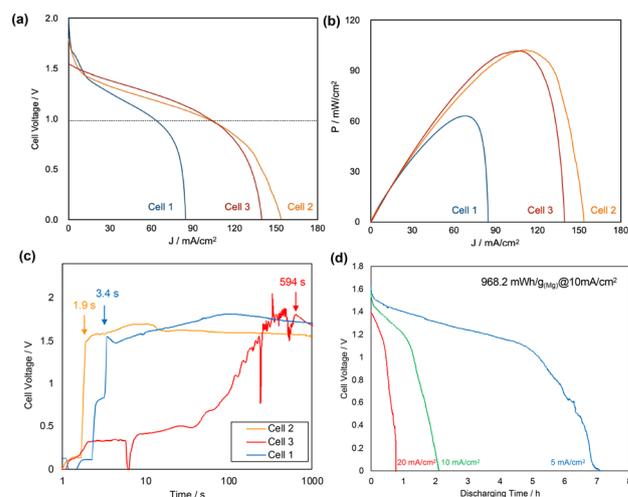

Fig. 2 I–V (a) and I–P (b) polarization curves of the cells (cell 1 (blue), cell 2 (yellow), and cell 3 (red)), time dependence of cell voltages of the cells after water activation (c), and discharge polarization curves of cell 2 at 5 (blue), 10 (green), and 20 mA cm⁻² (red) (d).

© 2024 The Author(s). Published by the Royal Society of Chemistry

RSC Appl. Interfaces, 2024, 1, 435–442 | 437

Table 1 Properties and performance of the cells

Entry no.	Cell 1	Cell 2	Cell 3
D_{paper} [g cm^{-3}]	0.56	0.45	0.31
$t_{incubation}$ [s]	3.4	1.9	594
Water uptake [mg]	232	302	448
OCV [V]	1.98	1.80	1.55
P_{max} [mW cm^{-2}]	63.0	103	102
J_{max} [mA cm^{-2}]	84.7	154	140
$J_{@1.0 V}$ [mA cm^{-2}]	61.8	100	101

Another important difference is that the incubation time to start electricity generation depended on the type of paper used. The filter paper and water-absorbing paper quickly absorbed water and started to generate electricity within 4 s (Fig. 2(c)), whereas the paper towel absorbed water slowly and it took 594 s to start generating electricity. Therefore, cell 2 was the most balanced battery in terms of high-power output and current generation starting quickly.

The discharge polarization curve at a current density of 10 mA cm^{-2} indicated a capacity density of 968.2 mW h g$_{(Mg)}^{-1}$, which was high enough for a paper battery (Fig. 2(d)). Most paper batteries have only achieved stable output at current densities of less than 1 mA cm^{-2}, whereas the present paper battery had a substantially higher output density comparable to sheet air batteries using liquid or gel electrolytes.

We compare our paper battery cells with mainly two types of paper batteries reported in the literature; one is the Zn–air type paper battery reported in the literature,[17] and the other one is the Mg–air paper battery reported in the literature[10] which use neutral electrolytes. The former one has low environmental impact because it does not use any toxic materials and uses a current collector with low amounts of metals; however, the output power density is too small (only 150 µW cm^{-2}). Our paper battery also does not use any toxic materials and uses safe and low-environmental impact carbon cathodes and a pigment electrocatalyst which has passed biotoxicity assesments,[23] but it shows 700 times higher power density (103 mW cm^{-2}) and *ca.* 1000 times higher in an optimal case (see the ESI,† S11).

Also, compared with the Mg–air battery, which uses high-cost silver current collectors, it showed 60 mW cm^{-2} in a previous paper.[9] However, we achieve 1.2 times higher power density without using current collectors and almost doubled power density with using a Cu mesh as a current collector, which costs lower than silver, due to the high ORR activity of the originally developed electrocatalyst. The selection criteria for electrolytes are as follows. Generally, in metal–air batteries, it is common to use alkaline electrolytes where the negative electrode metal is prone to dissolution and sufficient activity of the ORR can be expected at the positive electrode. However, in this study, from the perspective of achieving environmentally friendly and disposable paper batteries, selecting alkaline electrolytes that may have adverse effects on the human body was avoided. We compared the performance of paper batteries of low environmental impact,

especially without using alkaline or acidic electrolytes because those hazardous electrolytes cannot be obtained easily in our daily life. Although a Zn–air type paper battery, which realized 102 mW cm^{-2} using 6 M KOH, has been reported,[24] if a neutral electrolyte is used, it would fail.[10] Also, if 6 M KOH comes into contact with the human body, skin tissues are immediately damaged and serious prognostic symptoms remain. In order to realize safe paper batteries, we believe that such hazardous high pH electrolytes should not be used. Instead, saline water was chosen as the electrolyte considering its environmental impact, accessibility, and the fact that Mg dissolves in neutral to weakly acidic electrolytes. Under alkaline conditions, Mg dissolves in the electrolyte, but it forms insoluble Mg(OH)$_2$ at the surface of the anode, therefore, alkaline electrolytes cannot be used for Mg–air battery cells. However, selecting neutral electrolytes for metal–air batteries is uncommon, mainly due to the rarity of catalysts exhibiting high ORR activity near neutral pH.[25] Fortunately, we have discovered an AZUL catalyst that shows high ORR activity near neutral pH, enabling us to overcome this issue and select a neutral electrolyte.

Additionally, regarding the influence of electrolyte dosage, as shown in Table 1, it has become evident that cell 3, with sufficient electrolyte retention thickness and low density, exhibits the highest performance. This indicates the essential requirement for electrodes to be adequately wetted by the electrolyte to achieve high performance. However, due to its large pore size resulting in weak capillary action and low water uptake, we concluded that cell 2, with the most balanced dosage and capillary action, is the most optimal.

Moreover, the cells shown in the above-mentioned literature studies use Pt/C as a cathode electrocatalyst. It is well-known that Pt/C has disadvantages such as resource constraints and high cost, and it often ignites spontaneously when it comes into contact with organic solvents like alcohol even though it shows good ORR activity. Such a hazardous, expensive, resource-limited material cannot be disposed of. We have also evaluated the same paper battery cell using Pt/C as an electrocatalyst for the cathode, and it has shown good performance the same as the AZUL electrocatalyst case, but it is very harmful because only a small amount of alcohol ignites fire due to the high reactivity of Pt/C (see the ESI,† S14). Therefore, in order to realize safe and disposable paper batteries, we believe that such hazardous high pH electrolytes should not be used especially for wearable devices.

Furthermore, for applications shown later in this manuscript such as a SpO$_2$ sensor or a GPS logger, any strong alkaline electrolytes are not available in the environment in which those devices are used. Therefore, it is not appropriate to compare the performance of neutral electrolyte paper batteries used in environments, where high alkaline electrolytes should not be used, with that of paper batteries using high alkaline electrolytes.

After immersion in the electrolyte, the discharge continued for 2–3 hours at room temperature. The voltage gradually decayed due to drying of the electrolyte, but when

the electrolyte was supplied again, the voltage was recovered (see the ESI,† S13). This property ensures at least several hours of energy supply for wearable devices with only one time activation with the electrolyte.

Furthermore, the paper battery has enough flexibility. The battery can work with bending over 90° as shown in the ESI,† S15.

To create a disposable battery with a low environmental impact, it is necessary to develop an integrated paper battery without positive current collectors or resin clips. We consider the use of copper to be problematic. Ultimately, we have achieved a paper battery that does not use a copper mesh as a current collector. The positive electrode consists only of carbon materials and electrocatalysts, while the negative electrode is composed solely of magnesium foil. To achieve this, a conductive layer was formed by mixing CNFs and a binder to replace the positive current collector and mechanically compressing the paper battery.

Fig. 3(a) shows a schematic illustration of the fabricated paper battery and photographs and an SEM image of the components. On the cathode side, a black conductive layer using CNFs (see the inset SEM image) was formed. Fig. 3(b) shows a photograph of the tree-like designed disposable paper battery. The whole material was fixed by compression by using a needleless stapler and generated electricity after injection of salt water at the bottom (ESI,† S10). The output characteristics of this paper battery were OCV = 1.72 V, P_{max} = 76 mW cm^{-2}, and I_{max} = 154 mA cm^{-2} (Fig. 3(b)). Although these values were slightly lower than those of a battery with current collectors, the output was still much higher than those of existing paper batteries. This decrease in performance was attributed to the increased resistance of the cathode. Electrochemical impedance spectroscopy measurements showed that without current collectors, both the electrode resistance and electrolyte resistance increased because the lack of current collectors increased the electrode resistance and the addition of CNFs produced a denser electrode structure, hindering the electrolyte diffusion (see the ESI,† S7).

From the discharge polarization curves with different current densities (Fig. 3(c)), the cell capacity was 330.5 mW h $g_{(Mg)}^{-1}$ at a discharge of 10 mA cm^{-2}, which was about one-third of the capacity with the current collector case. However, when the discharge was decreased to 5 mA cm^{-2}, the capacity increased to 901.2 mW h $g_{(Mg)}^{-1}$, which was nearly equivalent to the capacity with current collectors. This suggests that the paper battery retained almost ideal cell capacity under these conditions. The high-performance paper battery realized the following reasons. We developed a high-performance ORR catalyst based on FeAzPc even under neutral pH conditions. This has not been achieved before by using MnO_2 and other electrocatalysts. We selected the optimum paper sheet for water absorption and activation of paper battery cells. For the current-collector-less paper battery case, we enhanced the electrical conductivity by adding CNFs.

To demonstrate the use of the water-activated paper battery in practical devices, we used the battery to power wearable devices of a patch SpO$_2$ sensor and a GPS sensor for sea-rescue. The patch pulse oximeter measures blood oxygen levels and pulse when it is attached to the body. However, for continuous monitoring, a thin, long-life power source is essential. The water-activated paper battery developed in this study is expected to provide sufficient power and capacity to drive the device when filled with saline solution.

Fig. 4 shows the SpO$_2$ sensor used in the experiment, along with the water-powered paper battery, and the demonstration of

Fig. 4 Photographs of cell components (a), a single paper battery cell (b), SpO$_2$ sensor (c), SpO$_2$ sensor with the cell (d), injection of salt water to the cell (e), and the active SpO$_2$ sensor (other side compared with panels (d) and (e)) (f). Real-time monitoring of O$_2$ saturation and pulse measured in a person (g).
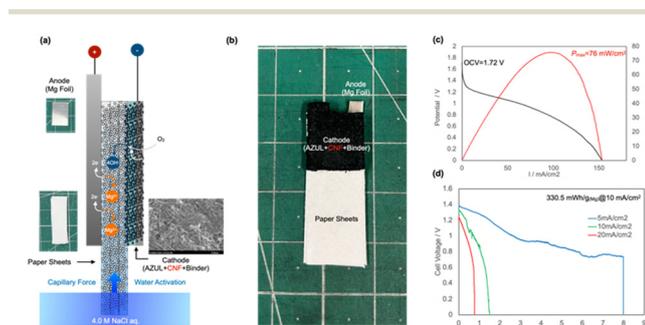

Fig. 3 Schematic of a completely disposable water-activated paper battery cell (a), a photograph of a disposable water activated paper battery (b), and its I–V/I–P polarization curves (c) and discharge polarization curves at different current densities (d), respectively. The inset in (a) shows an SEM image of the cathode containing CNFs.
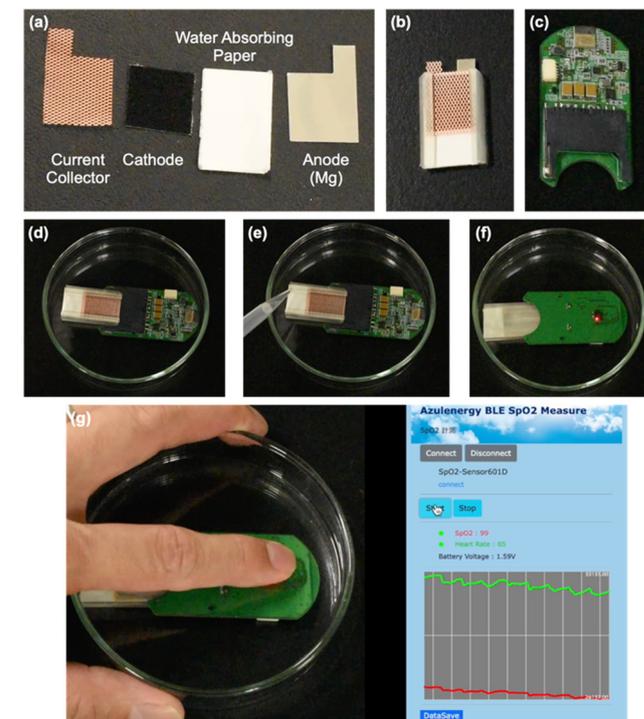
its operation. The SpO$_2$ sensor has Bluetooth communication capabilities, allowing blood oxygen levels to be monitored remotely on a PC or mobile device when measurements are initiated. The SpO$_2$ sensor has an SD card-shaped slot as the power supply unit, where a thin battery can be inserted for operation. The paper battery was inserted into the pulse oximeter's slot, absorbing saline solution to match its shape, and the pulse oximeter was attached to the body to confirm whether it could measure blood oxygen levels and pulse at a frequency of 1.0 Hz. The SpO$_2$ sensor obtained blood oxygen concentration signals with no interruptions. From the discharge polarization curves shown in Fig. 2(d), the output voltage decreased from *ca.* 1.8 to 0.9 V after 5.45 h discharging at a current density of 5.0 mA cm^{-2}. The cathode surface area of the paper battery cell was fixed at 1.0 cm^2, and the device running time was equal to the discharging time when the battery voltage reached 0.9 V. Additionally, we also demonstrated SpO$_2$ sensor activation using current-collector-free paper battery cells (see the ESI,† S12).

Additionally, we powered a GPS sensor with the paper battery. During water-based activities, a GPS sensor that transmits location information when a person is submerged can be crucial for waiting for sea rescue. The water-powered paper battery serves as a power source for both the submersion sensor and the GPS signal transmission. We connected three paper batteries in series inside a case to power the GPS logger, which was then attached to a life jacket as a submersion sensor (Fig. 5(a)). When the paper batteries became wet with sea water due to submersion, the GPS signal was successfully transmitted, accurately marking the location on Google Earth (Fig. 5(b)). This demonstrates that the paper battery developed in this study could function as both a submersion sensor and a power source. For life saving, the survival rate of victims of marine disasters decreases significantly after 72 h (3 days); therefore, the victim location should be traceable for at least 3 days. The energy consumption of the device was measured and only 276.3 mA h (= 828.9 mW h) was used when the telecommunication frequency was one signal per 120 s. This value and the paper battery capacity (968.2 mW h g^{-1}) suggested that it is sufficient to use only *ca.* 1 g Mg foil for the paper battery anodes when three serial battery cells are used.

Conclusions

The paper batteries developed in this study are not only disposable but are also expected to have a low environmental impact after disposal. Metal–air batteries normally use heavy metals, such as platinum and manganate compounds, as cathode catalysts for performance, so even if the amount of heavy metal used is small, the battery cannot be disposed of as is because of the safety and environmental impact compared with other battery systems.[26–28] In addition, it is difficult to achieve sufficient performance with other alternative safe catalysts. FeAzPc is a metal phthalocyanine analogue, a pigment widely used as a blue paint, and its safety has been confirmed by Ames tests and acute toxicity tests in fish.[23] The other electrode materials used are carbon and Mg alloys, which do not contain environmentally harmful heavy metals. NaCl is also used as the electrolyte, and in Mg–air batteries, Mg dissolves in the electrolyte to form magnesium salts, which are abundant in nature, particularly in seawater. These paper battery cells can be recharged by replacing the used anode Mg with a new one. This "mechanical charge" is one of the advantages of metal–air battery cells. The use of a biodegradable polymer, polylactic acid, for components like battery packaging, would allow natural hydrolysis, so only carbon, naturally occurring metal salts, and trace amounts of safe iron complexes remain in the end. Therefore, the paper battery developed in this study is expected to be a fully disposable, sustainable battery.[29]

Methods

Materials

FeAzPc (29*H*,31*H*-tetrapyrido[2,3-*b*:2′,3′-*g*:2″,3″l:2‴,3‴-*q*]porphyrazine iron complex) was synthesized according to the literature.[16,18,30] The same batch of FeAzPc was used throughout the study. KB (EC-300J) was purchased from Lion Specialty Chemicals, Co., Ltd. (Tokyo, Japan). Mg foil (0.03 × 100 × 100 mm) was purchased from NIRACO, Co., Ltd. (Tokyo, Japan). The Mg sheet (100 × 300 × 0.2 mm) was purchased from AS One Corporation (Osaka, Japan). 20% Pt/C was purchased from Sigma-Aldrich (USA). 20% Nafion® dispersion solution (DE2020 CS), dimethyl sulfoxide (DMSO), isopropyl alcohol (IPA), and other solvents were purchased from Fujifilm Wako Chemical Industry, Inc. (Osaka, Japan). Three types of paper sheets were purchased from Tamura Shokai, Co., Ltd., Nagaoka, Japan (entry 1), ADVANTEC, Tokyo, Japan (entry 2), and Nippon Paper CRECIA, Co., Ltd., Tokyo (KIMTOWEL, entry 3).
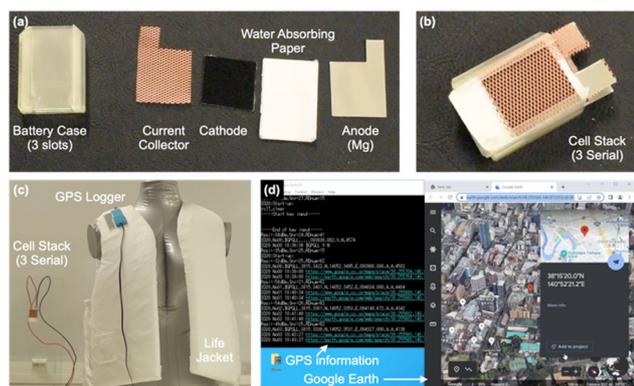

Fig. 5 Photographs of the cell components (a), the cell stack with three serial paper battery cells (b), and the arrangement of GPS loggers and the cell stack (c). A capture of the desktop showing the GPS information from the GPS logger activated by the cell stack with salt water and the detailed information obtained from Google Earth *via* GPS information (d).

Multi-layer CNTs with diameters of 20–60 nm and lengths of 0.5–2.0 mm were purchased from Koatsu Gas Kogyo.

Fabrication of paper batteries

The AZUL electrocatalyst was prepared according to the literature.[20] Typically, FeAzPc was dissolved in DMSO, and then KB was mixed into the solution and dispersed by sonication with a probe homogenizer (UD-200, TOMY SEIKO Co., Ltd., Japan). During the dispersion, FeAzPc was adsorbed into the KB, and then the dispersion was filtered and washed with DMSO to remove excess non-adsorbed FeAzPc. Catalyst ink (2.5 wt% catalyst) was prepared by mixing the AZUL electrocatalyst (1 g), 20% Nafion dispersion (1.8 mL) in IPA (36 mL), and deionized water (9 mL) in a planetary ball mill (P-6, Fritsch Japan, Co., Ltd., Yokohama, Japan) using zirconia balls and pots. Mg foil (99.99%, NIRACO, Co., Ltd.) or a Mg sheet (AZ31, AS One Corporation, Osaka, Japan) was fixed with paraffin onto the paper sheet, and then the back of the paper was coated with the catalyst ink by spray coating (SimCoat, Sono-Tek Corporation, NY, US).

Structural analysis

Surface scanning electron microscopy (SEM) images of the paper samples were obtained (S-5200, Hitachi High Technologies, Co., Ltd., Hitachi, Japan). To obtain the SEM images, the paper samples were cut with scissors and coated with Os by using an Os sputterer (HPC-1SW, Shinku Device, Inc., Saitama, Japan). The sample was immobilized on a sample stage with carbon tape for SEM observations.

Electrochemical measurements

The catalyst ink was dropped onto a glassy carbon electrode (BAS, Inc., Tokyo, Japan) to form a catalyst layer with a catalyst density of 300 $\mu g \ cm^{-2}$. A Pt wire and an Ag/AgCl electrode were inserted into the electrolyte as reference and counter electrodes, respectively. The rotating ring-disc electrode (RRDE) measurements for each catalyst were performed with an RRDE system (RRDE-3A, ALS Co., Ltd.) equipped with a bipotentiostat (2325, ALS Co., Ltd.).

The potential *vs.* Ag/AgCl was converted to the reversible hydrogen electrode (RHE) scale using the following equation.

$$E(vs. \ \text{RHE}) = E(vs. \ \text{Ag/AgCl}) + 0.197 + 0.059 \ \text{V·pH}$$

I–*V* polarization curves and discharge polarization curves were measured with potentiostats (Versastat-3 and Versastat-4, AMETEK, Berwyn, PA, USA).

Application to a wearable SpO$_2$ measurement device

A wearable SpO$_2$ sensor was fabricated by T&H Design, Co., Ltd., Fukushima, Japan. Detailed specifications are shown in the ESI,† S4. The SpO$_2$ sensor is slim (thickness <5 mm) and can be attached to the body to measure oxygen saturation and pulse. The sensor allows real-time monitoring when it is paired with a smartphone or PC *via* Bluetooth. The battery connector is SD card-shaped, and it can be powered by an SD card-sized battery.

We used a 3D printer (Form3$^+$, Formlabs, Inc., Somerville, MA, USA) to create a SD card-sized battery case. A paper battery with a Cu mesh as the collector was inserted into the battery case and the whole unit was inserted into the battery connector of the SpO$_2$ sensor.

Wetting the paper with 4 M NaCl aq. initiated power generation, and then the device was turned on and connected to a PC for real-time monitoring of oxygen saturation and pulse at a sampling rate of 1.0 Hz. The process was recorded as a video using an iPhone 11. Additionally, as a reference experiment, we measured the oxygen saturation and pulse using a commercially available SpO$_2$ sensor.

Application to a GPS logger

A wearable GPS logger was fabricated by T&H Design, Co., Ltd. Detailed specifications are shown in the ESI,† S5. A life jacket was provided by Amphico, Co., Ltd. (London, UK). The battery case for the cell stack was fabricated in the same way as that for the SpO$_2$ sensor by using a 3D printer. The cell was connected to the GPS logger with codes. Wetting the paper with 4 M NaCl aq. initiated power generation, and then, the device was automatically turned on and connected to a PC *via* a low-power wide-area Wi-Fi system for real-time monitoring of the location by using the GPS signal. The location logging information was visualized by Google Earth.

Author contributions

H. Y. conceived the idea of the work, conducted the whole part of the research, and wrote the whole part of the manuscript. Kosuke Ishibashi fabricated the paper battery cells and measured their performance. J. K. fabricated the smart life jacket. S. O. provided the CNFs. Koju Ito fabricated the SpO$_2$ sensor and the GPS logger.

Conflicts of interest

There are no conflicts to declare.

Acknowledgements

References

1 Z.-Y. Gu, X.-T. Wang, Y.-L. Heng, K.-Y. Zhang, H.-J. Liang, J.-L. Yang, E. H. Ang, P.-F. Wang, Y. You, F. Du and X.-L. Wu, *Sci. Bull.*, 2023, **68**, 2302.

2 X.-T. Wang, Z.-Y. Gu, E. X. Ang, X.-X. Zhao, X.-L. Wu and Y. Liu, *Interdes. Mater.*, 2022, **1**, 417.

3 T. Juqu, S. C. Willenberg, K. Pokpas and N. Ross, *Adv. Sens. Energy Mater.*, 2022, **1**, 100037.

© 2024 The Author(s). Published by the Royal Society of Chemistry

RSC Appl. Interfaces, 2024, **1**, 435–442 | 441

4 T. H. Nguyen, A. Fraiwan and S. Choi, *Biosens. Bioelectron.*, 2014, **54**, 640–649.

5 X. Yan, A. Xu, L. Zeng, P. Gao and T. Zhao, *Energy Technol.*, 2018, **6**, 140–143.

6 L. Zhang, M. Zhou, D. Wen, L. Bai, B. Lou and S. Dong, *Biosens. Bioelectron.*, 2012, **35**, 155–159.

7 C. W. Narváez Villarrubia, C. Lau, G. P. M. K. Ciniciato, S. O. Garcia, S. S. Sibbett, D. N. Petsev, S. Babanova, G. Gupta and P. Atanassov, *Electrochem. Commun.*, 2014, **45**, 44–47.

8 M. Hilder, B. Winther-Jensen and N. B. Clark, *J. Power Sources*, 2009, **194**, 1135–1141.

9 Y. Wang, H. Kwok, W. Pan, H. Zhang and D. Y. C. Leung, *J. Power Sources*, 2019, **414**, 278–282.

10 Y. Wang, W. Pan, S. Luo, X. Zhao, H. Y. H. Kwok and D. Y. C. Leung, *Int. J. Energy Res.*, 2022, **46**, 137–146.

11 H. Zhang, S. Hwang, M. Wang, Z. Feng, S. Karakalos, L. Luo, Z. Qiao, X. Xie, C. Wang, D. Su, Y. Shao and G. Wu, *J. Am. Chem. Soc.*, 2017, **139**, 14143–14149.

12 M. Grewal, Y. Matsuo and H. Yabu, *New J. Chem.*, 2021, **45**(14), 19228.

13 H. Yabu, K. Ishibashi, M. S. Grewal, Y. Matsuo, N. Shoji and K. Ito, *Sci. Technol. Adv. Mater.*, 2022, **23**, 31–40.

14 K. Ishibashi, M. S. Grewal, K. Ito, N. Shoji, Y. Matsuo and H. Yabu, *Adv. Energy Sustainability Res.*, 2022, 2200107.

15 D. Raptis, A. Ploumistos, E. Zagoraiou, E. Thomou, M. Daletou, L. Sygellou, D. Tasis and P. Lianos, *Catal. Today*, 2018, **315**, 31–35.

16 J. Shui, M. Wang, F. Du and L. Dai, *Sci. Adv.*, 2015, **1**, 1–8.

17 A. Poulin, X. Aeby and G. Nyström, *Sci. Rep.*, 2022, **12**, 1–8.

18 X. Wang, B. Wang, J. Zhong, F. Zhao, N. Han, W. Huang, M. Zeng, J. Fan and Y. Li, *Nano Res.*, 2016, **9**, 1497–1506.

19 J. Yang, F. Toshimitsu, Z. Yang, T. Fujigaya and N. Nakashima, *J. Mater. Chem. A*, 2017, **5**, 1184–1191.

20 H. Abe, Y. Hirai, S. Ikeda, Y. Matsuo, H. Matsuyama, J. Nakamura, T. Matsue and H. Yabu, *NPG Asia Mater.*, 2019, **11**, 57.

21 H. Yabu, K. Nakamura, Y. Matsuo, Y. Umejima, H. Matsuyama, J. Nakamura and K. Ito, *ACS Appl. Energy Mater.*, 2021, **4**, 14380–14389.

22 K. Ishibashi, K. Ito and H. Yabu, *APL Energy*, 2023, **1**, 016106.

23 *A 96-hour Acute Toxicity Study in Fish*, Receipt Number 662–19-E-9150, Study Number 99150, CERI, Kurume, Japan, 2020; *Ames tests*, K01–7234, CERI, Hida, Japan, 2020.

24 H. Zhang, B. Zhang, Y. Yang, D. Ye, E. Chen, Q. Liao and X. Zhu, *Chem. Commun.*, 2021, **57**, 1258–1261.

25 Z. Wang, Z. Lu, Q. Ye, Z. Yang, R. Xu, K. Kong, Y. Zhang, T. Yan, Y. Liu, Z. Pan, Y. Huang and X. Lu, *Adv. Funct. Mater.*, 2024, 2315150.

26 G. Li, G. Meng, Q. Liu, L. Feng, J. Luo, X. Liu, Y. Luo and P. K. Chu, *Adv. Powder Mater.*, 2024, **3**, 100154.

27 D. Qin, J. Ding, C. Liang, Q. Liu, L. Feng, G. Hu, J. Luo and X. Liu, *Acta Phys.-Chim. Sin.*, 2024, **40**, 2310034.

28 H. Zhang, G. Meng, Q. Liu, Y. Luo, M. Niederberger, L. Feng, J. Lio and X. Liu, *Small*, 2023, **19**, 2303165.

29 N. R. Aishwarya and P. Charan, *IJRASET*, 2023, **11**(2), 1015.

30 Y. Hirai, B. Sawano, T. Takaki and H. Yabu, *J. Nanosci. Nanotechnol.*, 2017, **18**, 455–458.